

# Evaluation of Moisture Sorption and Diffusion Characteristics of Asphalt Mastics Using Manual and Automated Gravimetric Sorption Techniques

Alex K. Apeageyi, PhD, PE, MASCE<sup>1</sup>; James R. A. Grenfell, PhD, MIHT, MIMMM<sup>2</sup> and Gordon D. Airey<sup>3</sup>, PhD, CEng, MIHT, MASCE<sup>3</sup>

<sup>1</sup>Research Fellow, Nottingham Transportation Engineering Centre, Department of Civil Engineering, University of Nottingham, University Park, Nottingham NG7 2RD, United Kingdom; email: alex.apeageyi@nottingham.ac.uk

<sup>2</sup>Research Officer, Nottingham Transportation Engineering Centre, Department of Civil Engineering, University of Nottingham, University Park, Nottingham NG7 2RD, United Kingdom; email: james.grenfell@nottingham.ac.uk

<sup>3</sup>Professor, Nottingham Transportation Engineering Centre, Department of Civil Engineering, University of Nottingham, University Park, Nottingham NG7 2RD, United Kingdom; email: gordon.airey@nottingham.ac.uk

**Abstract:** One of the most important factors influencing the durability of asphalt mixtures is moisture-induced damage resulting from the presence and the transport of moisture in pavements. Moisture-induced damage is an extremely complicated phenomenon that is not completely understood but believed to be governed by the interaction of moisture with asphalt mix components (mastic and aggregates). The objective of this study was, therefore, to characterize the sorption and diffusion characteristics of asphalt mastic using gravimetric vapor sorption techniques. Moisture transport, in the hygroscopic region, in asphalt mastics was studied using both static and dynamic gravimetric vapor sorption techniques to determine equilibrium moisture uptake and diffusion coefficients as a function of aggregate and filler types. For the 25-mm diameter thin asphalt mastic films and the testing conditions (23°C and 85% relative humidity) considered, the kinetics of moisture uptake obtained were characteristic of Fickian diffusion with a concentration-dependent diffusion coefficient. Equilibrium moisture uptake and diffusion coefficient estimated from the static measurements were comparable and of the same order of magnitude as those from dynamic sorption techniques. Both measurement techniques ranked the mixes similarly which suggest either method could be used to characterize moisture transport in asphalt mastics. Equilibrium moisture uptake was relatively higher in mixtures containing granite aggregates compared with limestone aggregate. In contrast, the diffusion coefficient of limestone aggregate mastics was higher than granite. Thus an inversely proportional relationship exists between moisture uptake and diffusivity of the asphalt mastics studied. The results suggest moisture transport is a function of aggregate type and that both equilibrium moisture uptake and diffusion coefficient are useful in studying moisture susceptibility in asphalt mixtures. The effect of mineral filler type on diffusion coefficient was minimal in the mastics containing granite aggregate but relatively high in mastic samples containing limestone aggregates. Diffusion coefficient was found to increase with sample thickness which was unexpected because diffusion coefficient (in an isotropic material) is considered an intrinsic property that is independent of sample size. The results suggested anisotropic diffusivity can occur in asphalt mastics and could be attributed to factors including mineralogy, microstructure, air voids, and the tendency of the aggregates to settle at the bottom of asphalt mastic with time. In addition to characterizing moisture transport in asphalt mastics, the results presented in this paper will be useful as inputs for numerical simulation of moisture damage in asphalt mixtures.

CE Database subject headings: Asphalts, Asphalt pavements, Material Properties, Water, Diffusion

Author keywords: Moisture diffusion, Diffusion Coefficient, Asphalt Mastics, dynamic vapor sorption, relative humidity, limestone, granite, Fick's law

## 52 **Introduction**

53 The transport of moisture into and/or through asphalt mastic is of great interest because it has relevance to  
54 the physico-chemical characterization, numerical modeling, and fundamental understanding of the  
55 moisture-induced damage phenomenon in asphalt mixtures, which is important for designing durable  
56 bituminous pavements. A key parameter that characterizes moisture transport in a material is the moisture  
57 diffusion coefficient. The effects of the presence and transport of moisture within asphalt mixtures is a  
58 leading cause of moisture damage that is a major cause of pavement distress. This is because the loss of  
59 cohesion within and / or the loss of adhesion between asphalt mastic and aggregate are commonly regarded  
60 as the principal causes of moisture-induced damage (Terrell 1994, Airey and Choi, 2006). The effects of  
61 moisture diffusion into the asphalt mastic as well as the effects of moisture on the adhesive bond between  
62 asphalt and aggregate are directly related to moisture diffusion characteristics of the mixture. Moisture can  
63 reach the asphalt-aggregate interface and cause stripping by diffusing through the asphalt or mastic. In  
64 addition, the moisture in the mastic can profoundly affect the rheology and engineering properties of the  
65 mastic (Cheng et al 2003). The mechanism of moisture-induced damage is currently not completely  
66 understood and therefore, empirical methods are currently the only commonly available means of studying  
67 the phenomenon. The study of moisture diffusion, with its focus on molecular movement of water at the  
68 mastic aggregate interface, offers a more fundamental approach for better understanding of the moisture-  
69 induced damage problem than existing empirical characterization test methods.

70 Traditionally, the susceptibility of an asphalt mixture to moisture-induced damage has been  
71 evaluated using an index-based parameter such as stiffness or strength, obtained before and after specified  
72 simulated moisture-induced tests (Airey and Choi, 2002). While these traditional approaches have been  
73 successfully used to evaluate moisture susceptibility, these tests are empirical in nature, and therefore  
74 require experience before their results can be properly interpreted. Also, prediction based on such empirical  
75 tests could be contradictory for certain mixtures (Apeagyei et al. 2006). Furthermore, the methods do not  
76 address moisture-damage at a level that could enable a fundamental understanding of the problem because  
77 moisture transport characteristics of the mastic and aggregate components of asphalt mixtures have not  
78 been routinely evaluated. The lack of moisture transport data for asphalt mix components (mastics and  
79 aggregates) is a major hindrance to a fuller understanding of moisture damage in asphalt mixtures. The

80 problem of the limited number of studies focused on moisture transport in asphalt mastic is further  
81 compounded by the rather large variations in reported diffusion coefficient values as a result of the different  
82 testing conditions (temperature and relative humidity) and experimental approaches (gravimetric and  
83 psychrometric) used in their determinations (Table 1).

84 It can be seen from Table 1 that one technique that has been reported for evaluating moisture  
85 diffusion in asphalt mastic is the measurement of weight gain in specimens submerged under water at room  
86 temperature (Kassem et al. 2006 and Vasconcelos et al. 2006). The reported diffusion coefficient for these  
87 studies ranged from 10 to  $24 \times 10^{-12} \text{ m}^2/\text{s}$  at  $25^\circ\text{C}$ .

88 Another technique used to measure diffusion coefficient in some previous studies (Kringos et al.  
89 2008 and Arambula et al 2010) is a gravimetric method similar to what Vasconcelos and co-workers used  
90 but with specimens exposed to moisture vapor (15% and 85% RH). The reported moisture diffusion  
91 coefficient values ranging from 0.13 to  $0.36 \times 10^{-12}$  and  $254.0 \times 10^{-12} \text{ m}^2/\text{s}$  appear to differ significantly. It  
92 should be noted that while Kringos and co-workers assumed Fick's second law (unsteady state diffusion)  
93 to estimate diffusion coefficient, the set-up for Arambula and co-workers appears to satisfy Fick's first law  
94 (steady-state diffusion and hence moisture permeability coefficient). As previously mentioned and further  
95 discussed next, the differences in experimental set-up used in the past may have contributed to the  
96 differences seen in the reported diffusion coefficient values.

97 In general, moisture can be transported in a porous material in three different ways: 1) diffusion, 2)  
98 capillary flow, and 3) hydraulic flow, depending on moisture content and the driving potential. When  
99 moisture content of a material is in the hygroscopic region (0-95% RH) diffusion is the main mechanism  
100 of moisture flow with vapor pressure as the driving potential. Capillary flow is the dominant mode of  
101 moisture transport for moisture content in the super-hygroscopic region ( $95 < \text{RH} < 100$ ) and capillary  
102 pressure in the pores of the material is the driving potential. For materials with moisture content in the  
103 super-saturated region, hydraulic flow is governed by Darcy's law with external pressure gradient (air  
104 pressure, water pressure, or gravitation) as the driving potential. In the super-saturated region all capillaries  
105 have been filled and therefore, no capillary pressure exists. Thus, it can be argued that the differences in  
106 reported asphalt mastic diffusion coefficient are due to the differences in testing conditions (diffusion and  
107 capillary flow) used by different investigators.

108 This study looks at moisture diffusion in asphalt mastic using gravimetric sorption techniques  
109 assuming classical Case I or Fickian diffusion and contributes to the understanding of moisture damage by  
110 providing equilibrium moisture uptake and Fickian diffusion coefficients that are useful for micro-  
111 mechanical characterization as well as numerical simulation of moisture-induced damage in asphalt  
112 mixtures. The moisture transport properties obtained in this study will also be useful as inputs for numerical  
113 models that simulate moisture-induced damage in asphalt mixtures.

114 In the current work, water vapor transport in asphalt mastics was studied using both static and  
115 dynamic gravimetric vapor sorption techniques to determine equilibrium moisture uptake and diffusion  
116 coefficient as a function of two aggregate and filler types. Asphalt mastic and aggregate form the two main  
117 components of asphalt mixtures with the mastic acting as the adhesive that binds the aggregates together.  
118 It was expected that the results from testing the asphalt mastic, may be of use in better understanding of  
119 moisture movement and associated moisture-induced damage in asphalt pavements by identifying factors  
120 influencing moisture diffusion in asphalt mastics.

121

## 122 **Theory**

### 123 **Moisture Uptake Profiles**

124 A moisture uptake profile describes the relationship between the amount of moisture ( $M_t$ ) a hygroscopic  
125 material exchanges (absorbs or desorbs), at a given relative humidity and temperature, with time. If  $w_0$  is  
126 the initial (dry) mass of a given material and  $w_t$  is the mass after time  $t$ , then the moisture uptake can be  
127 computed as the ratio of the amount of moisture absorbed at a given time to the initial dry mass of the  
128 sample at the beginning of the test (Eq. 1).

$$129 \quad \text{Mass uptake (\%)} = M_t = \frac{w_t - w_0}{w_0} * 100 \quad (1)$$

130 For a material at given temperature and relative humidity, moisture uptake increases until it reaches a  
131 thermodynamic equilibrium at which point no further changes in moisture uptake occurs. The moisture  
132 content at thermodynamic equilibrium ( $M_\infty$ ) is called equilibrium moisture uptake. The time it takes a  
133 material to reach  $M_\infty$  as well as the ratio  $\frac{M_t}{M_\infty}$  provide important insights into moisture transport (diffusion  
134 rate).

135

136 **Fick's first law**

137 Considering moisture content as the potential for mass transfer through a unit area of a section of an  
138 isotropic material, the mass flow of moisture per unit area or flux (F) is given by Fick's first law (Eq. 2).

139 
$$F = -D \frac{\partial C}{\partial x} \quad (2)$$

140 where F is the mass flow of moisture per unit area ( $\text{kg/s} \times 1/\text{m}^2$ ), D is the effective diffusion coefficient  
141 ( $\text{m}^2/\text{s}$ ), C is the water concentration ( $\text{kg}/\text{m}^3$ ), and x is the distance (m) in the flow direction. If the  
142 concentration C of the system is changing, then Fick's second law is the applicable model estimating  
143 diffusion coefficient under a given experimental condition as discussed next.

144

145 **Determination of diffusion coefficient**

146 When a thin planar sample is maintained at a constant relative humidity and moisture sorption is  
147 occurring via the two planes ( $x=0$  and  $x=l$ ) of the sample and utilizing the kinetic sorption data, moisture  
148 diffusion coefficient can be determined based on the solution of Fick's second law (Eq. 3) for an infinite  
149 plate geometry under one-dimensional isothermal conditions assuming a constant diffusion coefficient,  
150 negligible swelling, initial conditions (Eq. 4) and boundary conditions (Eq. 5). The assumption of a thin  
151 plate means the majority of diffusion occurs in-plane and radial diffusion is negligible.

152

153 
$$\frac{\partial C}{\partial t} = D \frac{\partial^2 C}{\partial x^2} \quad (3)$$

154

155 
$$t = 0, C = C_0 \text{ for } 0 < x < l \quad (4)$$

156

157 
$$t > 0, C = C_1 \text{ for } x = l \text{ and } \frac{\partial C}{\partial x} = 0 \text{ for } x = 0 \quad (5)$$

158 where t is time, l is the sample thickness, C is the water concentration,  $C_0$  is the initial uniform water  
159 concentration, and  $C_1$  is the constant moisture concentration at the surface.

160 The solution to Eq. 3 under the aforementioned conditions is given by Eq. 6 (Crank, 1975) which  
161 can be solved numerically using the sorption data to obtain the diffusion coefficient of the mastics. This is

162 one of the most accurate models for predicting moisture diffusion coefficient and will be called the full-  
 163 form equation in this paper.

164

$$165 \quad \frac{M_t}{M_\infty} = 1 - \sum_{n=0}^{\infty} \frac{8}{(2n+1)^2 \pi^2} e^{-\frac{D(2n+1)^2 \pi^2 t}{l^2}} \quad (6)$$

166

167 where  $M_t$  is the amount of moisture absorbed after time  $t$ ,  $n$  is an integer, and  $M_\infty$  is the maximum  
 168 amount of absorbed moisture at the thermodynamic equilibrium under a given relative humidity and  
 169 temperature,  $D$  is the diffusion coefficient, and  $l$  is plate thickness.

170

### 171 **Simplified solutions to Fick's second law**

172 Assuming Fickian diffusion, Eq. 6 can be simplified (Crank, 1975) as shown in Eq. 7.

173

$$174 \quad \frac{M_t}{M_\infty} = \frac{4}{l} \sqrt{\frac{Dt}{\pi}} \quad (7)$$

175 Therefore, plotting  $\frac{M_t}{M_\infty}$  against  $\sqrt{t}$ , for a moisture content ratio of at least 0.5 yields a straight line which  
 176 could be used to estimate moisture diffusion coefficient using Eq. 8.

177

$$178 \quad D = \frac{S^2}{16} \pi l^2 \quad (8)$$

179

180 where  $S$  is the slope of the plot of  $\frac{M_t}{M_\infty}$  against  $\sqrt{t}$ , as described above.

181 Another simplified method, the half-time method, was employed to estimate diffusion coefficient of

182 asphalt mastics. From Eq. 6, if the time  $t_{0.5}$  is determined such that  $\frac{M_t}{M_\infty} = 0.5$ , then the value of  $\frac{t}{l^2}$  for

183 which  $\frac{M_t}{M_\infty} = 0.5$  is given by Eq. 9 from which the diffusion coefficient ( $D$ ) could be computed (Eq. 10).

$$184 \quad \frac{t_{0.5}}{l^2} = - \left( \frac{1}{\pi D^2} \right) \ln \left( \frac{\pi^2}{16} - \frac{1}{9} \left( \frac{\pi^2}{16} \right)^9 \right) \quad (9)$$

$$185 \quad D = 0.049 \left( \frac{t_{0.5}}{l^2} \right)^{-1} \quad (10)$$

186 The approximate methods referred to as the slope method (Eq.8) and half-time method (Eq. 10) together  
187 with the full-form solution (Eq. 6) were used to estimate moisture diffusion of asphalt mastics in this  
188 paper. The plots from the slope method were also used to verify whether diffusion in asphalt mastics is  
189 Fickian in nature as discussed next.

190

### 191 **Verification of Fickian diffusion**

192 In the preceding sections on diffusion coefficients, a basic assumption was that moisture diffusion in  
193 asphalt mastics is Fickian in nature. Therefore, it was necessary to evaluate this assumption using the  
194 measured sorption data obtained in this study in order to verify the assumption of Fickian diffusion.

195 Moisture diffusion in a material can be considered as Fickian if the kinetics of the moisture uptake  
196 satisfies certain important requirements (Comyn 1983, Crank 1975). First, a plot of  $\frac{M_t}{M_\infty}$  against  $\sqrt{t}$ , should  
197 yield a straight line initially, followed by a curve that is concave with the time axis. Similarly, uptake  
198 curves of  $\frac{M_t}{M_\infty}$  against  $\frac{\sqrt{t}}{l}$  (i.e. reduced sorption curves) should coincide, approximately, regardless of film  
199 thickness. Finally, plots of uptake were evaluated to investigate the concentration dependence of asphalt  
200 mastic diffusion coefficient.

201

## 202 **Materials and Methods**

### 203 **Materials**

#### 204 *Mastic components*

205 Limestone and granite aggregates were obtained from UK quarries. Previous studies (Airey et al., 2007)  
206 suggest these aggregates have significantly different susceptibility to moisture-induced damage under  
207 laboratory conditions. Therefore, it was expected that mastics made from the selected aggregates would  
208 show different sorption and diffusion characteristics. The aggregates were mechanically sieved in the  
209 laboratory to obtain only materials passing the 1-mm sieve and retained on 0.125-mm sieves (fine  
210 aggregate). The fine aggregate specific gravity values were 2.640 and 2.626, respectively, for the limestone  
211 and granite samples used (EN 12697, AASHTO T 84) which suggest the two aggregate types were similar  
212 in terms of density. Moisture absorption (EN 12697, AASHTO T84) for the limestone aggregates (0.70

213 percent) was relatively lower in magnitude than the granite (0.92 percent). The fine aggregate specific  
214 surface areas, determined using octane probe and a dynamic sorption device, were 2.57 m<sup>2</sup>/g and 3.49 m<sup>2</sup>/g  
215 for the limestone and granite, respectively.

216 In addition to the fine aggregates, limestone and granite mineral fillers satisfying BS EN 1097-7-  
217 2008 were used. Again the choice of the mineral fillers was done to quantify the effect if any, of different  
218 types of fillers used in asphalt mixtures.

219 A 40/60 penetration grade bitumen from a single source was used for preparing all the mastics. The  
220 use of a single binder type was justified based on data from previous studies on moisture-induced damage  
221 (Curtis et al. 1993) that suggested that aggregate chemistry is more influential than the composition of  
222 asphalt binders. Bituminous binders similar to the ones used in this study are the single most common  
223 binders used in the UK for asphalt concrete production and have been used to successfully study moisture-  
224 induced damage in the past. Since moisture diffusion in a material is mainly influenced, at the molecular  
225 level, by the physico-chemical properties of its constituents, it was expected that similar trends in moisture  
226 diffusion behaviour would be obtained for different binder/aggregate combinations.

### 227 *Mastic Mix Design*

228 The proportion of the constituent components (fine aggregate, mineral filler, bitumen) of the  
229 mastics was 50:25:25 by weight of mixture (Kringos et al. 2008). The aggregate components were weighed  
230 separately, combined and thoroughly mixed in a mixing bucket, and heated at the mixing temperature of  
231 185°C for about 10 minutes before adding hot bitumen (185°C) to the mixture. This relatively high mixing  
232 temperature was used because of the high amount (25% w/w) of mineral filler used that results in very  
233 viscous mixtures. The mixture was mixed using a Hobart mechanical mixer for about five minutes to  
234 produce a homogenous mastic samples. The mastic were put in quart tins and stored in temperature  
235 controlled (20°C, 50% RH) conditions until testing.

### 236 *Sorption Specimens*

237 Cylindrical disk specimens with nominal diameters of about 25 mm were used for evaluating the  
238 sorption and diffusion characteristics of the mastics. They were prepared by carefully pouring molten  
239 mastic (140°C) into specially designed silicone molds to form virtually void free specimens without any  
240 compactive effort been applied. The average bulk specific gravity of the mastic measured using AASHTO



241 T166 was 1.917 (compared with a theoretically computed value of 1.907) which support the voidless (0%  
242 air voids) assumption. The thickness of the specimens ranged from about 1.50 mm to about 5.50 mm. The  
243 dimensions used in this study encompassed those used in previous studies. The specimens were cooled to  
244 room temperature and stored in a desiccator (to keep dry) until testing.

245 Table 2 shows details of the experimental matrix used for the study including the type of tests  
246 conducted, the type of mastics tested and the number of samples tested. Overall more than 30 individual  
247 mastic specimens were fabricated and tested.

## 248 **Methods**

### 249 *Kinetic Vapor Sorption Profiles*

250 Kinetic vapor sorption profiles for asphalt mastic were obtained using two different moisture vapor  
251 gravimetric sorption techniques. The first method involved the use of saturated potassium chloride salt  
252 solution at 23°C to generate a relative humidity of approximately 85% in a desiccator jar and manually  
253 measuring the weight gain with time (desiccator method). The weight gain (moisture uptake) of the mastic  
254 specimens was measured periodically (daily) using a Precisa XR 305A balance (Precision Balance Services  
255 Ltd) with a 0.1µg resolution. The moisture uptake was monitored until ‘thermodynamic equilibrium’ (i.e.  
256 a change of 0.0001g over a 24 hour period) for the conditions in the desiccator jar. At least three mastic  
257 specimens of each mix type were tested.

258 Some drawbacks of the desiccator method include the frequent (daily) opening and closing of the  
259 container (with attendant loss of vapor pressure) and the labor intensive nature of the method. Also, because  
260 of the stagnant nature of airflow within the desiccator jar, the time required to reach equilibrium is high (1-  
261 3 weeks). Despite these shortcomings, the desiccator method is easy to use, relatively cheap to setup, and  
262 several replicate specimens could be tested at the same time.

263 The second gravimetric method used was a dynamic sorption one and involved the use of an  
264 environmental chamber to precisely generate and maintain 85% RH at a temperature of 23°C while  
265 continuously measuring the weight gain of the mastic samples as it adsorbs water vapor (environmental  
266 chamber method). A TAS Model 600FS LTCL Series 3 environmental chamber capable of maintaining  
267 temperatures ranging from -75°C to 180°C and relative humidity from 0 to 95% was used. Air flow in the  
268 chamber was estimated to be about 0.50 m/s (about 0.10 m/s near the specimen). A Vibra HT-230CE tuning

269 fork analytical balance with a resolution of 0.1 $\mu$ g with static resistant plastic shield (to shield the specimen  
270 from the high speed air flow in the environmental chamber) was used to continuously monitor moisture  
271 uptake. Weight gain data was stored automatically via an RS-232C & peripheral device output to a personal  
272 computer. During the test, weight gain was captured every minute for a period of about 200 hours until  
273 ‘thermodynamic equilibrium’. Compared to the desiccator method, the time to reach thermodynamic  
274 equilibrium was comparatively lower. The main advantage of the automated method includes the ability to  
275 dynamically monitor moisture uptake with higher accuracy in sorption profiles. The major drawback of the  
276 environmental chamber method is that only one sample could be tested at a time and it is relatively more  
277 expensive than the desiccator method.

278

## 279 **Results and Discussion**

### 280 **Moisture Uptake Profiles**

281 Moisture uptake profiles were computed as the ratio of moisture uptake at a given time to the original  
282 weight of the sample at the beginning of the test (Eq. 1). Sample moisture uptake results are presented in  
283 Figure 1 for the desiccator method and in Figure 2 for the climatic method. In both cases, moisture uptake  
284 increases rapidly at the beginning of the test and slows as “equilibrium” is approached. From Figure 1, it  
285 can be seen that the amount of moisture absorbed by asphalt mastic appears to be dependent on both  
286 thickness and aggregate type. Also the results suggest moisture uptake by mastic samples containing  
287 granite are relatively higher compared to limestone mixtures in most cases.

288         Similar to the results obtained for the desiccator method, differences in moisture uptake were seen  
289 based on the aggregate type in the climate chamber method. Mastic containing granite aggregate (GA) and  
290 / or granite filler (GF) exhibited moisture uptake profiles that plotted relatively higher than those containing  
291 limestone aggregates (Fig. 2).

292

293 Thus the trend in moisture uptake obtained from the desiccator method agrees with that obtained from the  
294 more accurate climate chamber method. However, the time to equilibrium moisture uptake appears to be  
295 shorter in the climatic chamber compared with the desiccator jar. The faster moisture uptake in the climate  
296 chamber could be attributed to several reasons related to the test set-up. First, the climate chamber method

297 is automated in terms of humidity generation and control. Secondly, the daily removal of specimens from  
298 the sealed desiccators for weighing affects the partial vapor pressure generated by the saturated KCl solution  
299 contained in the desiccator jar. Furthermore, unlike the desiccator method where the air around the sample  
300 is static, in the climate chamber, air was constantly circulated by a high powered electric fan (air flow speed  
301 = 0.5 m/s in the chamber).

### 302 **Equilibrium Moisture Uptake**

303 Equilibrium moisture uptake was computed as the maximum moisture uptake observed during a sorption  
304 test (maximum uptake from Figs. 1 and 2). The exponential nature of Eq. 6 suggests that an infinite amount  
305 of time is required for a sample to reach equilibrium moisture content. For practical reasons and since the  
306 sensitivity of the balance used in this study was 0.0001 g, it was assumed that a sample reaches  
307 “pseudoequilibrium” when the change in moisture uptake over a given 24 hour period does not exceed  
308 0.0002 g. The equilibrium moisture uptake for the different mastics for both the desiccator method and the  
309 climate chamber method are presented in Figure 3. Each value of moisture uptake in Fig. 3 is the arithmetic  
310 mean for three or more samples of each mastic type, measured under the same experimental conditions.

311 In both gravimetric methods (Fig 3a and 3b), the magnitude of equilibrium moisture uptake appears  
312 to be a function of aggregate type. Equilibrium moisture uptake was higher in the mastics containing granite  
313 aggregate than in those with limestone. Several reasons could be used to explain the relatively higher  
314 moisture absorption in the granite mastics. The results, showing that asphalt mastics containing granite  
315 aggregates can absorb more moisture than the mastic containing limestone, appear to be in agreement with  
316 the moisture absorption (obtained using AASHTO T 84) data previously presented for granite (0.9%) and  
317 limestone (0.7%) fine aggregates. Another possible explanation for the higher moisture uptake in the granite  
318 mastic could be attributed to the mineralogy of the aggregate. Granite is composed predominantly (about  
319 72%) of silicon dioxide – a material with strong affinity for water and sometimes used as a desiccant – and  
320 also alumina (about 14%) which previous studies (Fisher et al., 1922) suggest could absorb up to 18% of  
321 its weight in moisture. The differences in the microstructure of the aggregates used could be another  
322 possible reason for the differences in equilibrium moisture uptake obtained for the different asphalt mastics.  
323 As previously mentioned, specific surface energy of the granite fine aggregate used in this study was  
324 relatively higher than the limestone fine aggregate (3.49 m<sup>2</sup>/g versus 2.57 m<sup>2</sup>/g). Theoretically, the higher

325 the surface area of a material, the greater the potential sites for moisture vapor molecules to adhere to. The  
326 results of the current study as well those from previous studies (Fisher et al., 1922) suggest the asphalt  
327 mastic moisture uptake profiles (moisture diffusion and transport) depend on both mineralogical as well as  
328 microstructural characteristics of the constituent aggregates used. Therefore, both mineralogical and  
329 microstructural characteristics of mineral aggregates should have an important effect on moisture-damage  
330 susceptibility of asphalt mixtures.

### 331 **Verification of Fickian diffusion**

333 Asphalt mastic diffusion characteristics presented in this paper were based on the assumption that Fickian  
334 diffusion is applicable. It was therefore, necessary to verify the assumptions to assure the validity of the  
335 results as discussed next. Moisture diffusion in a material can be considered as Fickian if the kinetics of the  
336 moisture uptake satisfies certain important requirements (Comyn 1983, Crank, 1975).

337 First, a plot of  $\frac{M_t}{M_\infty}$  against  $\sqrt{t}$ , should yield a straight line initially, followed by a curve that is  
338 concave with the time axis. Figure 4 depicts sample plots obtained for three mastics containing limestone  
339 aggregate and limestone filler showing linear relationship between  $\frac{M_t}{M_\infty}$  and  $\sqrt{t}$  that suggest diffusion in  
340 asphalt mastic might be Fickian in nature. Similar relationships were obtained for the other mixtures  
341 considered.

342

### 343 **Determination of Diffusion Coefficient**

344 Diffusion coefficient for the various mastics was determined using both the full-form solution and the  
345 simplified solutions. Determination of diffusion coefficient using the full-form solution utilized Eq. 6 and  
346 a numerical optimization routine by minimizing the sum of squares between the predicted moisture uptake  
347 and the measured uptake. For the simplified methods, Eq. 8 and Eq. 10 for the slope method and half-time  
348 method, respectively, were used to estimate diffusion coefficient of the mastics. It was observed (Figure 5)  
349 that both the simplified methods and the full-form solution of Fick's second law gave essentially the same  
350 results. The results suggest the two methods, full solution and half-time method could be used  
351 interchangeably to estimate diffusion coefficient of asphalt mastics.

352 Table 3 lists a summary of the average mastic moisture diffusion coefficients grouped in terms of  
353 mastic type, specimen thickness, equilibrium moisture uptake, and gravimetric sorption technique. The  
354 effects that these factors may have on mastic moisture diffusion coefficient are discussed next.

355  
356 **Factors influencing diffusion coefficient of asphalt mastics**

357 One objective of this study was to identify factors that influence moisture diffusion in asphalt mastics in  
358 order to better understand moisture damage in asphalt mixtures. Four factors were considered including  
359 aggregate type, mineral filler type, specimen thickness, and moisture uptake (concentration). The  
360 importance of the first two factors (aggregate type and filler type) on moisture diffusion is obvious even  
361 though their effect on the actual mechanism of moisture damage is not clear. The third factor was important  
362 to consider because the diffusion coefficient determined in this study is expected to be used as input for  
363 numerical simulation of moisture damage in asphalt pavements and therefore any thickness effect  
364 (anisotropy), if any, needs to be documented. It is generally assumed that diffusion coefficient is an intrinsic  
365 material property that is independent of thickness but this has not been verified for asphalt mastics in  
366 previous studies. One assumption of Fickian diffusion is that diffusion coefficient is concentration  
367 dependent. Again this assumption has not been verified for asphalt mastics and therefore warrants this  
368 study.

369 ***Thickness effects***

370 The results of asphalt mastic diffusion coefficients determination are presented in Figures 5 and 6 where a  
371 plot of diffusion coefficient against specimen thickness are compared for different combinations of  
372 aggregate and filler types.

373 The results suggest asphalt mastic diffusion coefficient increases with increase in thickness (Fig.  
374 6) especially for the limestone aggregate mastic considered in this study. For specimen thickness less than  
375 4.0 mm, moisture diffusion in limestone mastic appears to be similar to that of granite. Given that both  
376 mastics in Fig. 6 contain the same limestone filler (LF), the results suggest that for thinner specimens, the  
377 type of mineral filler may be a key factor influencing moisture diffusion. At greater thickness, limestone  
378 aggregate mastics moisture diffusion are relatively higher than the corresponding granite mastic which  
379 demonstrate the dominate influence of aggregate type on moisture transport. The effect of aggregate

380 mineralogy and microstructure could account for the higher rate of moisture transport (higher diffusion  
381 coefficient) in limestone mastics. As previously discussed, the limestone fractions considered in this paper  
382 have lower specific surface area (and hence lower moisture storage/adhesion capacity) than granites. It is  
383 also known that limestone aggregates have very different pore size and pore distribution (dual porosity)  
384 than granite. The finer pores in granite allows greater amounts of moisture to be adsorb and may have  
385 contributed to the observed differences in diffusivity observed in this study.

386

### 387 *Mineral filler effects*

388 For mastic containing the same aggregate type, the influence of mineral filler type on  
389 moisture diffusion appears to be minimal (Fig. 7). It must be noted that the amount of filler used  
390 was half that of the aggregate used and thus could have a limiting influence on moisture  
391 transport. Since replacing mineral filler with an active filler (such as hydrated lime) is one  
392 proven way of improving moisture sensitivity of asphalt mixtures, the minimal effect of filler on  
393 mastic diffusion is unexpected and warrants additional studies to investigate the phenomenon.

394

### 395 *Longitudinal and radial diffusion*

396 As previously discussed, the apparent relationship between asphalt mastic diffusion coefficient and  
397 specimen thickness was unexpected. One reason could be that both radial and longitudinal (through the  
398 thickness) diffusion could be occurring at the same time due to factors such as anisotropy (caused by  
399 aggregate settling to the bottom of the specimen during the long duration testing) and the violation of one  
400 of the assumptions (thin samples) of Fickian diffusion. For a material undergoing both radial and  
401 longitudinal diffusion (i.e. where radial diffusion may not be negligible), Eq. 11 (Crank, 1975) may be  
402 applicable and therefore, a linear relationship may exist between effective diffusion coefficient  $D$   
403 (measured) and the square of specimen thickness ( $l$ ). Eq. 11 can therefore be used to 1) verify the existence  
404 of radial diffusion and 2) to estimate both radial and longitudinal diffusion coefficient components from  
405 the experimentally measured diffusion coefficient.

406

$$D = D_z + \left( \frac{2D_r}{\pi^2 a^2} \right) l^2 \quad (11)$$

407 where  $D_r$  = the radial or lateral diffusion coefficient

408  $D_z$  = the longitudinal diffusion coefficient

409  $a$  = radius of specimen

410 As shown in Figure 8, the relationship between  $D$  and  $l^2$  is approximately linear for most of the  
411 mastics tested. This demonstrates that both radial and longitudinal diffusion might be occurring in the  
412 asphalt mastics tested, especially in thicker specimens. The results (slope and intercept values) from Figure  
413 8 were used to estimate radial and longitudinal diffusivity of asphalt mastic as presented in Table 4. Because  
414 of the limited number of specimens tested, the results should be considered as tentative. It is interesting,  
415 however, to note the close agreement between the longitudinal diffusion coefficient obtained in this study  
416 ( $0.10$  to  $1.23 \times 10^{-12}$   $m^2/s$ ) and the corrected (both experimentally and numerically) diffusion coefficient  
417 values reported for similar mastics (approximately 1 mm thick) by Kringos et al. 2008. It is also interesting  
418 to note the similarity (in terms of order of magnitude) between radial diffusion coefficient ( $65$  to  $362 \times 10^{-12}$   
419  $m^2/s$ ) obtained in this study and reported aggregate diffusion coefficient in previous studies ( $122$  to  $200$   
420  $\times 10^{-12}$   $m^2/s$  by Kringos et al. 2008 and  $210$  to  $245 \times 10^{-12}$   $m^2/s$  reported by Arambula et al. 2010) which would  
421 suggest the radial diffusion observed in the current study may be due to aggregate particles that settles in  
422 the mastic as previously discussed.

423 Thickness-dependent diffusivity has not previously reported in asphalt mastics even though the  
424 phenomenon has been observed in other materials (Fernando et al., 2011; Pereira and Yarwood, 1996;  
425 Tutuncu and Labuza, 1996). Additional studies looking at radial and longitudinal diffusion in asphalt  
426 mastics is warranted. However, the limited data obtained in this study suggest anisotropic diffusivity in  
427 asphalt mastics. For homogenous and isotropic materials, diffusivity can be considered as an intrinsic  
428 property that is independent of size (sample thickness). The observed variation of diffusivity with thickness  
429 (resulting in apparent radial and longitudinal diffusivities) reported in this paper suggests asphalt mastic  
430 may not be isotropic and/or homogenous. The authors believe that asphalt mastic, under the laboratory  
431 conditions used during a typical gravimetric moisture diffusion experiment (isothermal condition, tests  
432 lasting 100s of hours), could result in significant settlement of the denser fine aggregate particles to the  
433 bottom of the sample leaving the lighter mineral filler components near the upper portions of the sample. It  
434 is conceivable that the settling aggregates could in turn result in pockets of minute cavities (air pockets) at

435 the original locations of the aggregate. The probability of these effects occurring would obviously increase  
436 with sample thickness. The consequence of these two changes is a mastic sample that can be considered as  
437 anisotropic (i.e. a graded material with most of the more porous aggregates settled at the bottom and lighter  
438 but less porous material near the top). These are further compounded by the fact that diffusion coefficient  
439 of aggregates ( $122$  to  $200 \times 10^{-12}$  m<sup>2</sup>/s [Kringos et al. 2008];  $80800 \times 10^{-12}$  m<sup>2</sup>/s [Henon et al. 2002]) and air  
440 ( $26000000 \times 10^{-12}$  m<sup>2</sup>/s) are significantly larger than that of asphalt binders and therefore any small changes  
441 in their amount could large effect on diffusivity of mastics.

#### 442 443 ***Concentration-dependent diffusion coefficient***

444 The concentration dependence of moisture diffusion in asphalt mastic was analyzed by plotting diffusion  
445 coefficient against equilibrium moisture uptake for the four different mastics considered in the study (Fig.  
446 9). In all cases, diffusion coefficient appears to decrease with increasing equilibrium moisture content. The  
447 relationship between moisture absorption and diffusion coefficient of asphalt mastics can thus be  
448 characterized by an inversely proportional function of moisture uptake and diffusivity. These results  
449 showing concentration-dependent coefficient of diffusion suggest moisture transport in asphalt mastics is a  
450 function of aggregate type and that both equilibrium moisture uptake and diffusion coefficient should be  
451 considered when characterizing moisture transport in asphalt mixtures. Some previous studies (Kringos et  
452 al. 2008; Chen et al. 2003) have suggested, based on the higher equilibrium moisture uptake and lower  
453 diffusion coefficient of granites, that equilibrium moisture uptake is more useful than the magnitude of  
454 diffusion coefficient for characterizing moisture susceptibility. The results of the current study showing  
455 concentration dependent diffusion coefficient suggest both parameters are complimentary and should be  
456 considered together when evaluating moisture diffusion in asphalt mixtures.

457

#### 458 ***Simulation of diffusion in asphalt mastics***

459 Moisture diffusion in asphalt mastics can be simulated using values of diffusion coefficient and equilibrium  
460 moisture uptake obtained in this study. Figure 10 and Figure 11 show sample plots of moisture diffusion in  
461 two of the mastic studied. A 4-mm thick specimen was assumed for both mastics. Diffusion coefficient was  
462 taken as  $2.043 \times 10^{-12}$  m<sup>2</sup>/s and  $1.697 \times 10^{-12}$  m<sup>2</sup>/s for mastics containing limestone (LA+LF) and granite



463 (GA+GF) mastic, respectively. The corresponding equilibrium moisture uptakes were 0.0994% and  
464 0.1459%, respectively for limestone and granite mastics. The plot illustrates differences in the rate as well  
465 as magnitude of equilibrium moisture uptake in mastics. For example, the plots show that after about 100  
466 hours and at a depth of 0.5 mm from the surface of the mastic specimen, about 0.068% of moisture had  
467 been absorbed in the limestone mastic compared to about 0.095% in the granite. Given that each of the  
468 mastic types illustrated in Figures 10 and 11 contained the same aggregate types, the results suggest it takes  
469 the granite mastic longer to reach equilibrium moisture content compared with limestone aggregate. The  
470 results appear to agree with previously reported values for moisture diffusion in asphalt mastic (Kringos et  
471 al. 2008).

472

### 473 **Summary and Conclusions**

474 This study was conducted to characterize the sorption and diffusion characteristics of asphalt mastic using  
475 gravimetric vapor sorption techniques. Moisture vapor sorption tests were conducted at 23°C and 85%  
476 RH on four asphalt mastics fabricated using the same pen 40/60 bitumen but two different aggregates and  
477 two different mineral filler types. The following conclusions were reached based on the results of the  
478 study.

- 479 • The kinetics of moisture uptake obtained was characteristic of Fickian diffusion with a  
480 concentration-dependent diffusion coefficient.
- 481 • Equilibrium moisture uptake and diffusion coefficient estimated from the static measurements  
482 were comparable and of the same order of magnitude as those from dynamic sorption techniques.  
483 Both measurement techniques ranked the mixes similarly which suggest either method could be  
484 used to characterize moisture transport in asphalt mastics.
- 485 • Equilibrium moisture uptake was relatively higher in mixtures containing granite aggregates  
486 compared with limestone aggregate. In contrast, the diffusion coefficient of limestone aggregate  
487 mastics was higher than granite. Thus the relationship between moisture absorption and diffusion  
488 coefficient of asphalt mastics can be characterized by an inversely proportional function of  
489 moisture uptake and diffusivity. The results suggest moisture transport is a function of aggregate

490 type and that both equilibrium moisture uptake and diffusion coefficient are useful in studying  
491 moisture susceptibility in asphalt mixtures.

- 492 • The effect of mineral filler type on diffusion coefficient was minimal in the mastics containing  
493 granite aggregate but relatively high in mastic samples containing limestone aggregates.
- 494 • Diffusion coefficient was found to increase with sample thickness which was unexpected because  
495 diffusion coefficient (in an isotropic material) is considered an intrinsic property that is  
496 independent on sample size. The results suggested anisotropic diffusivity can occur in asphalt  
497 mastics and could be attributed to factors including mineralogy, microstructure, air voids, and the  
498 tendency of the aggregates to settle at the bottom of asphalt mastic with time.
- 499 • In addition to characterizing moisture transport in asphalt mastics, the results presented in this  
500 paper will be useful as inputs for numerical simulation of moisture damage in asphalt mixtures.

501

502 **Acknowledgements**

503 The authors acknowledge the assistance of the following Nottingham Transportation Engineering Centre  
504 personnel: Martyn Barrett, Richard Blakemore, Nancy Milne, Lawrence Pont, Jonathan Watson, and  
505 Michael Winfield for material testing. The funding for this project was provided in part by the UK  
506 Engineering and Physical Sciences Research Council (EPSRC).

507

508 **References**

509 Ahmad, N. Asphalt mixture moisture sensitivity evaluation using surface energy parameters. PhD. Thesis.  
510 University of Nottingham, 2011.

511 Airey, G.D., Masad, E., Bhasin, A., Caro, S. and Little, D. Asphalt mixture moisture damage assessment  
512 combined with surface energy characterization. In Proceedings of a Conference on Advanced  
513 Characterization of Pavement and Soil Engineering Materials (Loizos A, Scarpas T and Al-Qadi  
514 IL (eds)), 2007.

515 Airey, G.D. and Choi, Y.K. State of the Art Report on Moisture Sensitivity Test Methods for Bituminous  
516 Pavement Materials. Road Materials and Pavement Design, Vol. 3, Issue 4, 2002, pp. 355-372.

517 Apeageyi, A.K., Buttlar, W.G., and Dempsey, B.J. Moisture Damage Evaluation of Asphalt Mixtures  
518 using AASHTO T283 and DC(T) Fracture Test. Proceedings of the 10th International Conference  
519 on Asphalt Pavements, International Society of Asphalt Pavement, Quebec, Canada, 2006, pp.  
520 740-751.

521 Arambula, E., Caro, S., and Masad, E. Experimental Measurement and Numerical Simulation of Water  
522 Vapor Diffusion through Asphalt Pavement Materials. Journal of Materials in Civil Engineering,  
523 Vol. 22 Issue 6, 2010, 588–598.

524 Chen, D.X, Little, D.N, Lytton, R.L., and Holste, J.C. Moisture Damage Evaluation of Asphalt Mixture  
525 by Considering both Moisture Diffusion and Repeated-Load Conditions. In Transportation  
526 Research Record, Journal of the Transportation Research Record, No. 1832, Transportation  
527 Research Board of the National Academies, Washington, D.C., 2003, pp. 42-49.

528 Comyn, J. Durability of Structural Adhesives. Kinloch, A.J. Ed. Applied Science Publishers, New York,  
529 1983. P.84.

530 Curtis, C. W., R. L. Lytton, and C. J. Brannan. Influence of Aggregate Chemistry on the Adsorption and  
531 Desorption of Asphalt, Transportation Research Record, No 1362, 1 –9, 1992.

532 Crank, J. The Mathematics of Diffusion, 2nd ed.; Oxford University Press: New York, 1975; pp 414.

533 Terrel, R. L. Water Sensitivity of Asphalt-Aggregate Mixes, SHRP-A-403, 1994.

534 Fernando, W.J.N., Low, H.C., and Ahmad, A.L. (2011). Dependence of the effective diffusion coefficient  
535 of moisture with thickness and temperature in convective drying of sliced materials. A study on  
536 slices of banana, cassava and pumpkin. Journal of Food Engineering, Vol. 102 pp. 310–316.

537 Fisher H. L., Faust, H. L., and G.H. Walden. Alumina as an absorbent for water in organic combustions.  
538 The Journal of Industrial and Engineering Chemistry, Vol. 14, No. 12. 1922, pp. 1138.

539 Faust, H. L., and G. H. Walden. Alumina as an absorbent for water in organic combustions. The Journal  
540 of Industrial and Engineering Chemistry, Vol. 14, No. 12. 1922, pp. 1138.

541 Henon, F. E., Carbonell R. G., and J. M. DeSimone. Effect of polymer coatings from CO<sub>2</sub> on water-vapor  
542 transport in porous media. AIChE Journal, Vol. 48, No. 5. 2002, pp. 941-952.

543 Kassem, E. A., Masad, E., Bulut, R., and Lytton, R. L. Measurements of Moisture Suction and diffusion  
544 coefficient in Hot-mix asphalt and their Relationships to moisture damage. In Transportation  
545 Research Record, Journal of the Transportation Research Record, No. 1970, Transportation  
546 Research Board of the National Academies, Washington, D.C., 2006. pp. 45–54

547 Kringos, N., Scarpas, A., and deBondt, A. Determination of Moisture Susceptibility of Mastic-Stone  
548 Bond Strength and Comparison to Thermodynamical Properties. Journal of the Association of  
549 asphalt Paving Technology, Vol. 77, 2008. pp. 435-478.

550 Pereira, M. R., and Yarwood, J. (1996). ATR-FTIR spectroscopic studies of the structure and  
551 permeability of sulfonated poly(ether sulfone) membranes. 2: Water diffusion processes. J. Chem.  
552 Soc., Faraday Trans., 92(15), 2737–2743.

553 Tutuncu, M.A., and Labuza, T.P. (1996). Effect of geometry on the effective moisture transfer diffusion  
554 coefficient. Journal of Food Engineering, Vol. 30, pp. 433–447.

555 Vasconcelos, K. L., Bhasin, A., Little, D. N., and Lytton, R.L. Experimental Measurement of Water  
556 Diffusion through Fine Aggregate Mixtures. Journal of Materials in Civil Engineering Vol. 23  
557 Issue 4, 2011. pp. 445-452.

558 **List of Tables**

559 Table 1. Sample reported asphalt mastic diffusion coefficients

560 Table 2. Experimental matrix

561 Table 3. Longitudinal and radial diffusion coefficient of asphalt mastic

562

Table 1. Sample reported asphalt mastic diffusion coefficients

Reference	Blend proportions (by weight)	$D \times 10^{-12}$ ( $m^2/s$ )	Specimen characteristics and experimental conditions
Kassem et al. (2006)	Aggregate: 52.4% sandstone, 35.0% igneous screening, 4.6% hydrated lime asphalt: 8.0% PG 76-22	10.26	Cylindrical specimens, 50 mm in diameter and 50 mm in height, sitting in a shallow water bath at 25°C, while measuring the change in the logarithm of total suction using a psychrometer embedded in the middle specimen and placed 5 mm above the bottom end of the of the specimen. Aggregate size passing sieve Number 16 (1.18mm). Air voids not specified.
	Aggregate: 66.2% natural sand, 25.8% limestone sand asphalt: 8.0% (PG 64-22 & PG 64-28)	9.72 & 24.30	
Kringos et al. 2008	Aggregate: 50% crushed sand, 25% lime asphalt: 25% binder (Pen 70/100, Cariphalt XS, Sealoflex)	0.13 – 3.08	Gravimetric sorption method applied to 30 mm × 30 mm and 1 mm thick specimens placed inside an 85% relative humidity chamber at 25°C. Aggregate size (top size 1.18 mm). Air voids not specified.
Arambula et al. (2010)	Aggregate: 47.3% diabase, 42.5% sand, 1.7% dust asphalt: 8.5% PG 70-22	25444	Gravimetric method (ASTM E96, wet cup/dry cup method) applied to cylindrical ensembles containing 70 mm diameter and 4–5 mm thick specimens, where the ensembles were placed in a chamber with 15% relative humidity at 35°C. Aggregate size passing sieve No. 4 (4.75 mm). Air voids between 11–13%. Used Fick's first law to estimate D.
Vasconcelos et al. (2011)	Aggregate: N/A, asphalt: 8.9% (PG 58-XX, XX=10, 22, 28)	0.78 – 2.23	23.9 °C temp. Conditioning by submerging in water for 21 months and measuring SSD with time using a sensitive mass balance. Aggregate size passing sieve 1.18 mm sieve. Air voids between 7–11%. Specimen size 12 mm diameter by 50 mm thick.
	Aggregate: N/A asphalt: 8.9% (PG 58-XX, XX=10, 22, 28)	2.21 – 4.90	37.8 °C temp. Conditioning by submerging in water for 14 months and measuring SSD with time using a sensitive mass balance. Aggregate size passing sieve 1.18 mm sieve. Air voids between 7–11%. Specimen size 12 mm diameter by 50 mm thick.

N/A = data not available

566 Table 2. Experimental matrix

Matic type	Test method	No. specimens tested	<sup>1</sup> Thickness (mm)
LA + LF	Desiccator jar	8	3.19 ± 1.50
	Environmental chamber	3	3.37 ± 1.04
LA + GF	Desiccator jar	6	2.63 ± 1.08
	Environmental chamber	3	4.22 ± 0.50
GA + LF	Desiccator jar	3	3.93 ± 1.09
	Environmental chamber	3	3.37 ± 0.27
GA + GF	Desiccator jar	3	4.32 ± 0.71
	Environmental chamber	3	3.53 ± 0.98

LA = Limestone aggregate, LF = limestone filler, GA = granite aggregate, GF = granite filler. All mastics contained 40/60 pen bitumen. <sup>1</sup> = Mean ± SD

567  
568

569  
570

Table 3. Moisture diffusion coefficient of asphalt mastics at 23°C based on desiccator and climatic chamber methods.

Matic type	Test method	No. specimens tested	<sup>1</sup> Thickness (mm)	Equilibrium moisture uptake (%)	Diffusion coefficient x 10 <sup>-12</sup> (m <sup>2</sup> /s)
LA + LF	Desiccator jar	8	3.19 ± 1.50	0.1136 ± 0.025	4.02 ± 5.09
	Climatic chamber	3	3.37 ± 1.04	0.0738 ± 0.023	2.59 ± 0.22
LA + GF	Desiccator jar	6	2.63 ± 1.08	0.1236 ± 0.023	1.33 ± 0.74
	Climatic chamber	3	4.22 ± 0.50	0.0811 ± 0.006	4.75 ± 0.06
GA + LF	Desiccator jar	3	3.93 ± 1.09	0.1211 ± 0.032	2.04 ± 1.07
	Climatic chamber	3	3.37 ± 0.27	0.1095 ± 0.001	2.87 ± 0.01
GA + GF	Desiccator jar	3	4.32 ± 0.71	0.1198 ± 0.022	2.17 ± 0.48
	Climatic chamber	3	3.53 ± 0.98	0.1484 ± 0.022	2.44 ± 0.22

LA = Limestone aggregate, LF = limestone filler, GA = granite aggregate, GF = granite filler. All mastics contained 40/60 pen bitumen. <sup>1</sup> = Mean ± standard deviation

571



572 Table 4. Longitudinal and radial diffusion coefficient of asphalt mastic

Matic type	Test method	No. specimens tested	<sup>1</sup> Thickness (mm)	Long Diffusion coefficient x 10 <sup>-12</sup> (m <sup>2</sup> /s)	Radial Diffusion coefficient x 10 <sup>-12</sup> (m <sup>2</sup> /s)
LA + LF	Desiccator jar	8	3.19 ± 1.50	1.23 ± 1.61	361.57 ± 87.18
	Climatic chamber	3	3.37 ± 1.04	0.09 ± 0.23	173.12 ± 14.00
LA + GF	Desiccator jar	6	2.63 ± 1.08	0.37 ± 0.20	101.99 ± 17.91
	Climatic chamber	3	4.22 ± 0.50	0.48 ± 0.55	206.72 ± 25.71
GA + LF	Desiccator jar	3	3.93 ± 1.09	0.18 ± 0.26	95.66 ± 12.01
	Climatic chamber	3	3.37 ± 0.27	0.45 ± 2.19	242.18 ± 159.08
GA + GF	Desiccator jar	3	4.32 ± 0.71	0.70 ± 0.53	64.84 ± 22.64
	Climatic chamber	3	3.53 ± 0.98	0.51 ± 0.06	122.92 ± 3.69

LA = Limestone aggregate, LF = limestone filler, GA = granite aggregate, GF = granite filler. All mastics contained 40/60 pen bitumen. <sup>1</sup> = Mean ± standard deviation

573  
574  
575  
576

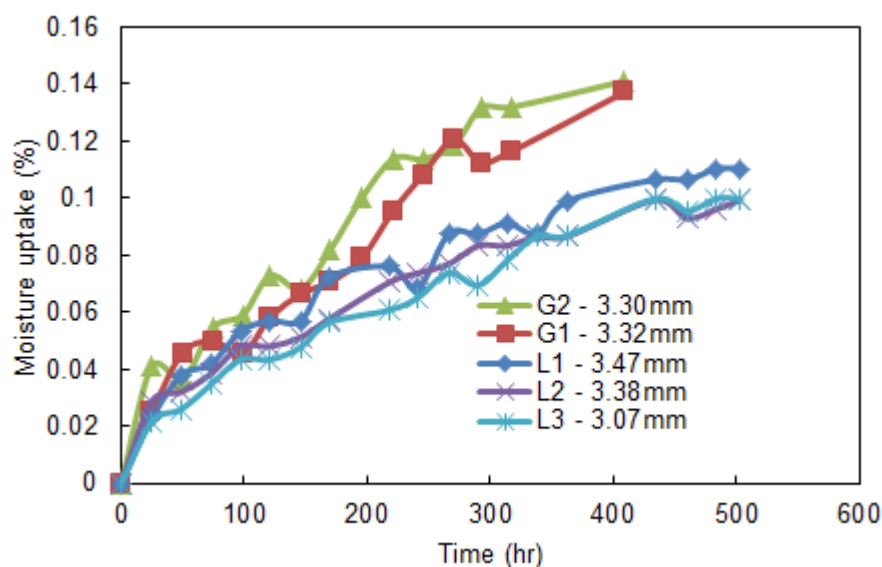
577

578 **List of Figures**

- 579 Fig. 1. Sample asphalt mastic moisture uptake profiles obtained using desiccator method. Moisture uptake for  
 580 mastics containing granite aggregate and filler (G1 and G2) were relatively higher than limestone aggregate and  
 581 filler (L1-L3) mastics. All specimens contained the same 40/60 pen asphalt binder and limestone mineral filler.  
 582 Fig. 2. Sample asphalt mastic moisture uptake profiles obtained using climate chamber method. Moisture uptake for  
 583 mastics containing granite (GA and GF) plotted relatively higher than limestone (LA and LF) mastics which seems  
 584 to agree quite well with the desiccator method.  
 585 Fig. 3. Equilibrium moisture uptake for asphalt mastic obtained from desiccator jar (a) and climate chamber (b)  
 586 methods. Each value of moisture uptake in Fig. 3 is the arithmetic mean for three or more samples of each mastic  
 587 type, measured under the same experimental conditions. The error bars represent  $\pm$  one standard deviation. LA+LF  
 588 = mastic with limestone aggregate and limestone filler. LA+GF = mastic with limestone aggregate and granite filler.  
 589 GA+LF = mastic with granite aggregate and limestone filler. GA+GF = granite aggregate with granite filler. All  
 590 mastics contained 40/60 pen bitumen.  
 591 Fig. 4. Values of  $\frac{M_t}{M_\infty}$  plotted against  $\sqrt{t}$  for asphalt mastic gives a straight line for  $\frac{M_t}{M_\infty} < 0.6$  suggesting Fickian  
 592 diffusion. Values plotted were obtained from three replicates of the same mastic.  
 593 Fig. 5. Estimation of diffusion coefficient for asphalt mastic using simplified and full-term solutions. Half-time  
 594 method agrees better with full-term solution than slope method. Data shown are for 19 different mastic specimens.  
 595 Fig. 6. Effects of aggregate type and specimen thickness on moisture diffusion of asphalt mastics containing the  
 596 same limestone mineral filler (LF).  
 597 Fig. 7. Effects of mineral filler type on asphalt mastic diffusion coefficient. For the same aggregate type (limestone,  
 598 LA; or granite, GA, neither the limestone filler (LF) nor the granite filler (GF) significantly altered moisture  
 599 diffusion in asphalt mastic.  
 600 Fig. 8. Investigation of radial and longitudinal diffusion in asphalt mastic. Linear relationship between diffusion and  
 601 thickness suggest both modes of diffusion occurs in mastics.  
 602 Fig. 9. Plots of diffusion coefficient against equilibrium moisture uptake showing linearly decreasing diffusivity  
 603 with moisture content for four different asphalt mastic types. The results demonstrate moisture diffusion in asphalt  
 604 mastic is concentration dependent.  
 605 Fig. 10. Simulation of moisture diffusion in asphalt mastic containing limestone aggregate and limestone filler.  
 606 Testing conditions simulated included 85% RH at a temperature of 23°C for moisture content ranging from about 0  
 607 to 0.10%. Plotted values are moisture uptake (%).  
 608 Fig. 11. Simulation of moisture diffusion in asphalt mastic containing granite aggregate and granite filler. Testing  
 609 conditions simulated included 85% RH at a temperature of 23°C for moisture content ranging from about 0 to  
 610 0.15%. Plotted values are moisture uptake (%).

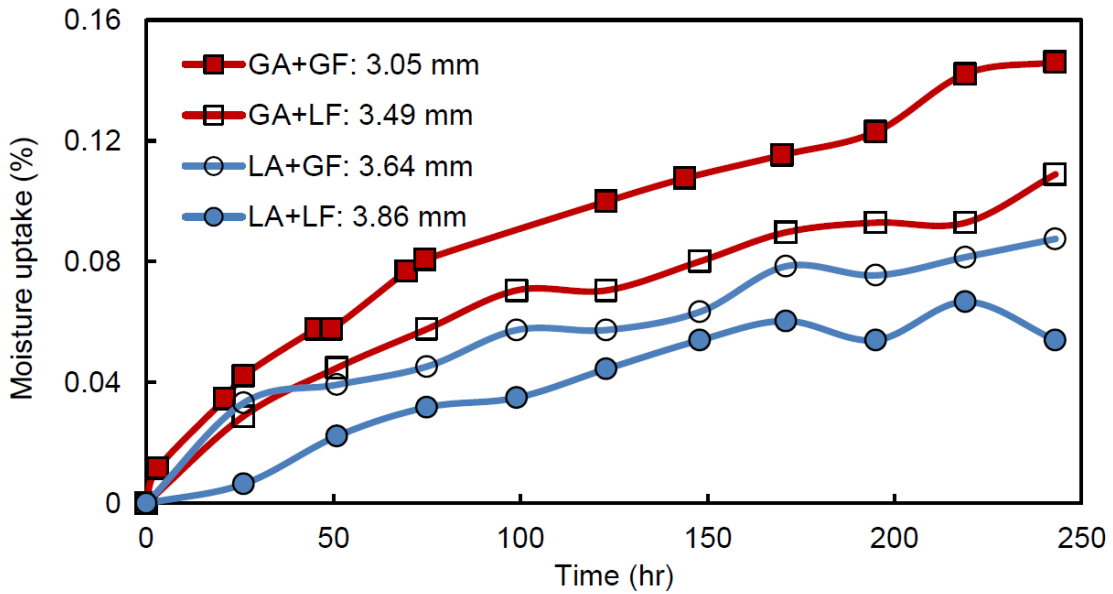
611

612 **FIGURES**

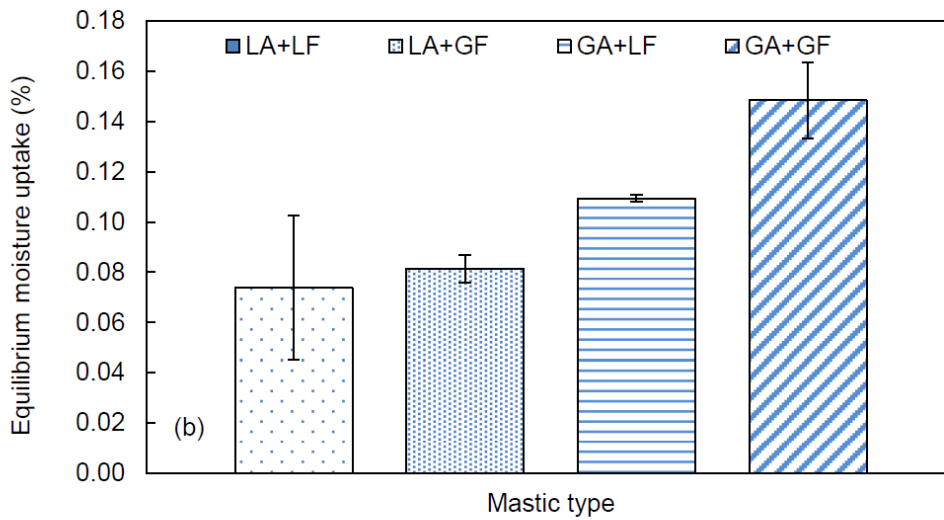
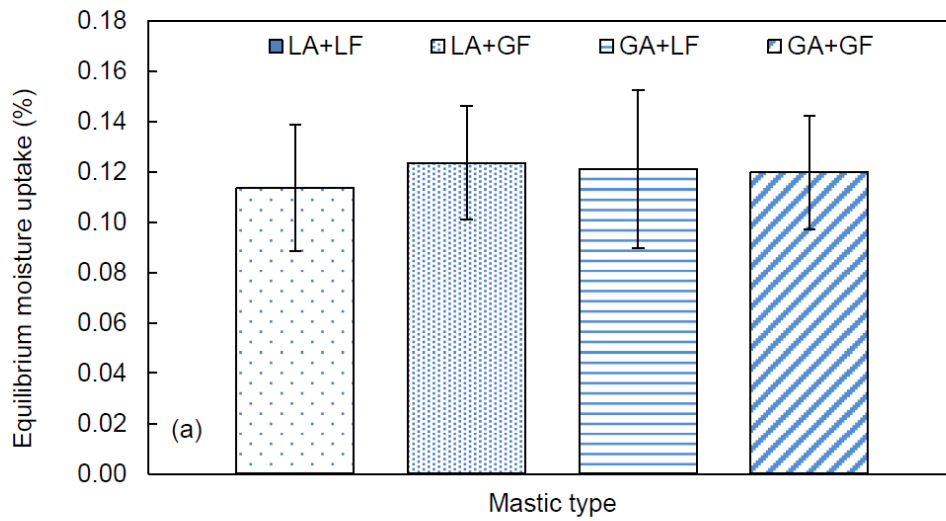


613

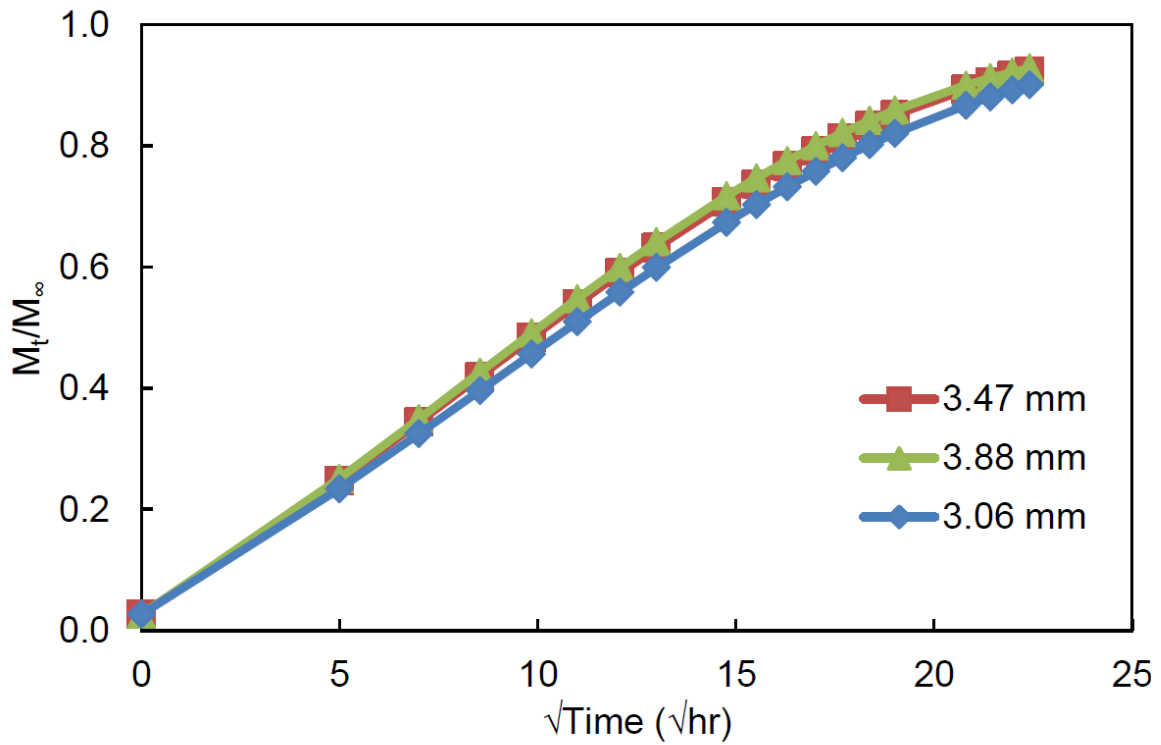
614 Fig. 1. Sample asphalt mastic moisture uptake profiles obtained using desiccator method. Moisture uptake for  
 615 mastics containing granite aggregate and filler (G1 and G2) were relatively higher than limestone aggregate and  
 616 filler (L1-L3) mastics. All specimens contained the same 40/60 pen asphalt binder and limestone mineral filler.  
 617



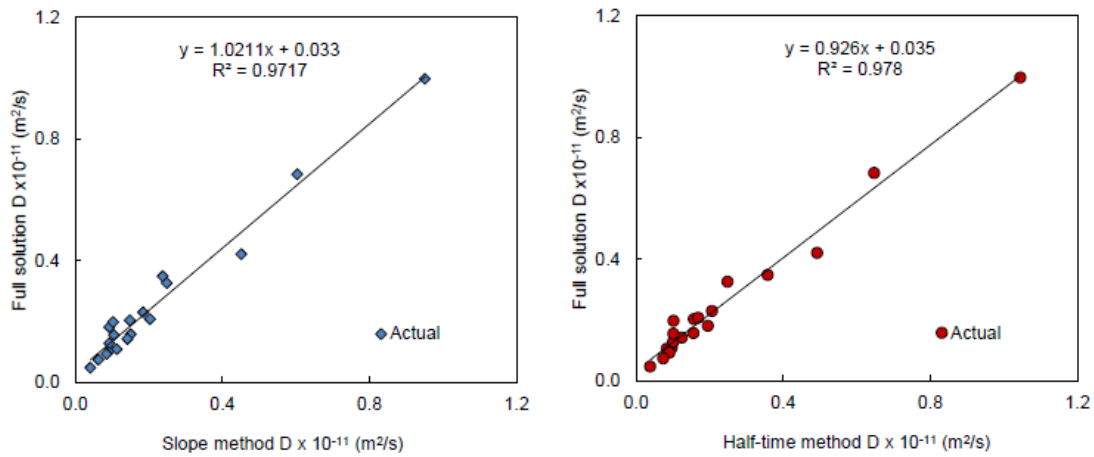
618 Fig. 2. Sample asphalt mastic moisture uptake profiles obtained using climate chamber method. Moisture uptake for  
 619 mastics containing granite (GA and GF) plotted relatively higher than limestone (LA and LF) mastics which seems  
 620 to agree quite well with the desiccator method.  
 621



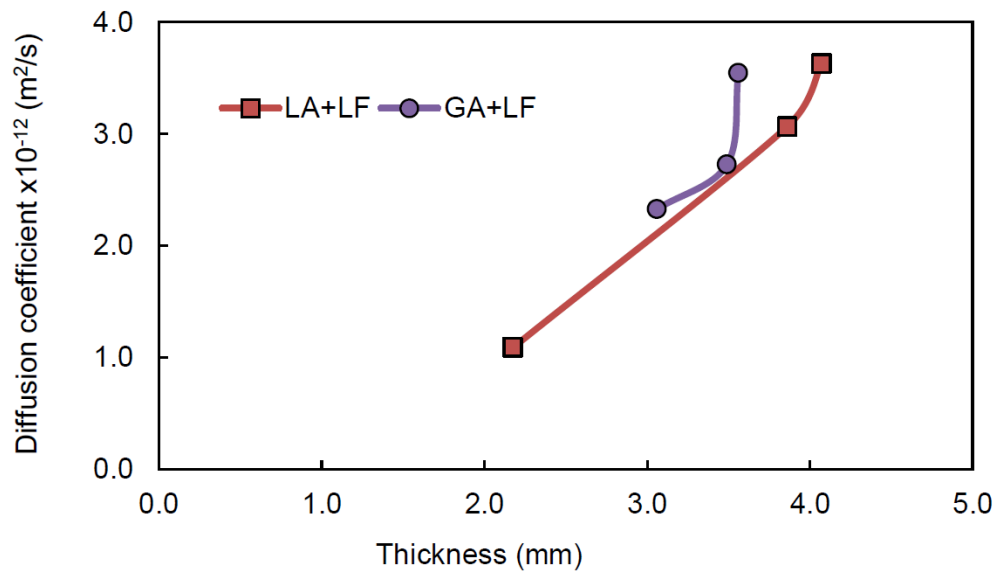
622 Fig. 3. Equilibrium moisture uptake for asphalt mastic obtained from desiccator jar (a) and climate chamber (b)  
 623 methods. Each value of moisture uptake in Fig. 3 is the arithmetic mean for three or more samples of each mastic  
 624 type, measured under the same experimental conditions. The error bars represent  $\pm$  one standard deviation. LA+LF  
 625 = mastic with limestone aggregate and limestone filler. LA+GF = mastic with limestone aggregate and granite filler.  
 626 GA+LF = mastic with granite aggregate and limestone filler. GA+GF = granite aggregate with granite filler. All  
 627 mastics contained 40/60 pen bitumen.  
 628



629  
 630 Fig. 4. Values of  $\frac{M_t}{M_\infty}$  plotted against  $\sqrt{t}$  for asphalt mastic gives a straight line for  $\frac{M_t}{M_\infty} < 0.6$  suggesting Fickian  
 631 diffusion. Values plotted were obtained from three replicates of the same mastic.  
 632

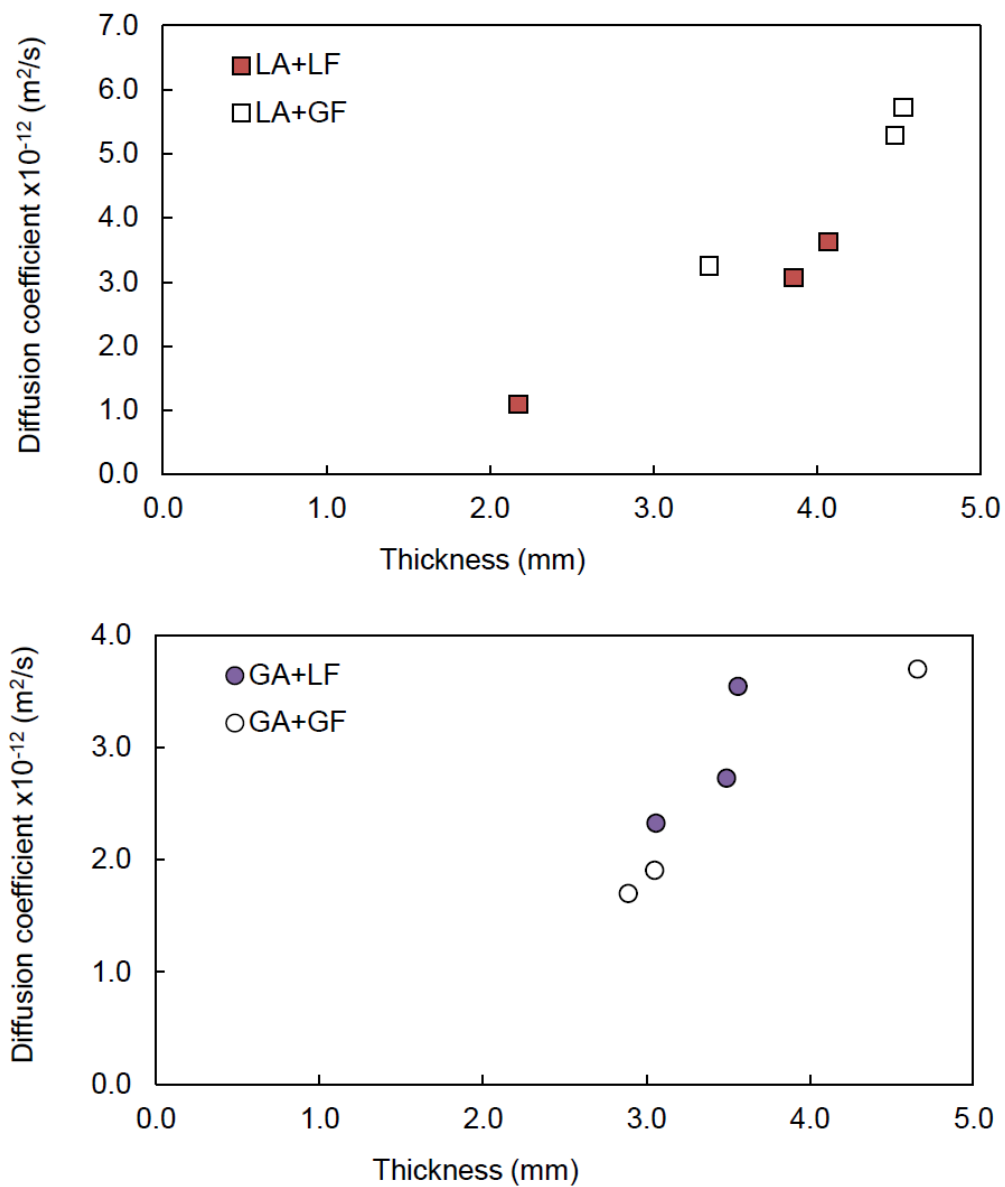


633  
 634 Fig. 5. Estimation of diffusion coefficient for asphalt mastic using simplified and full-term solutions. Half-time  
 635 method agrees better with full-term solution than slope method. Data shown are for 19 different mastic specimens.  
 636

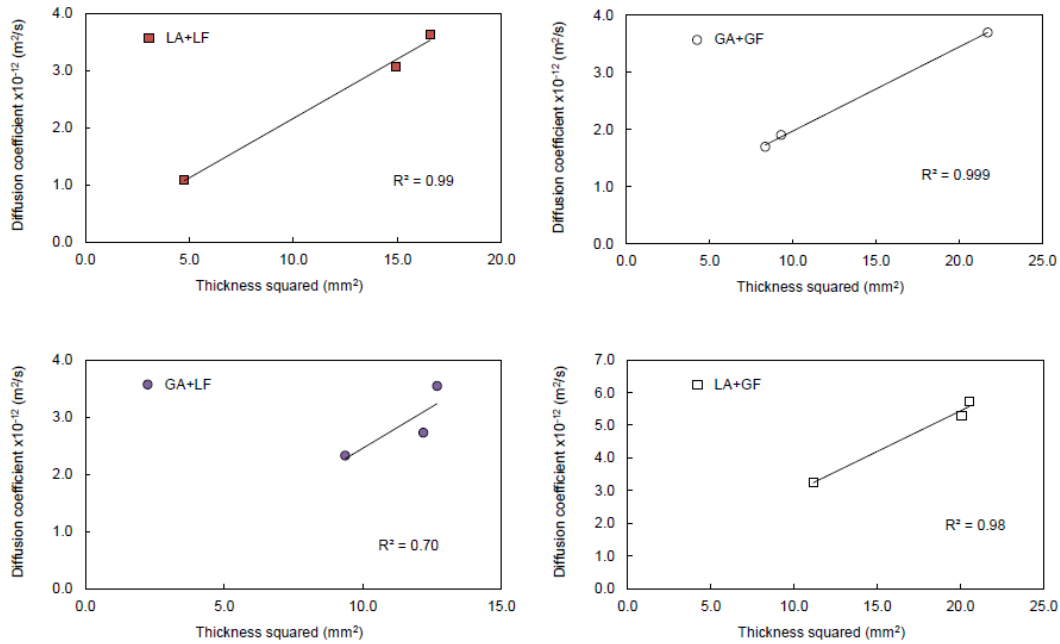


637  
638  
639

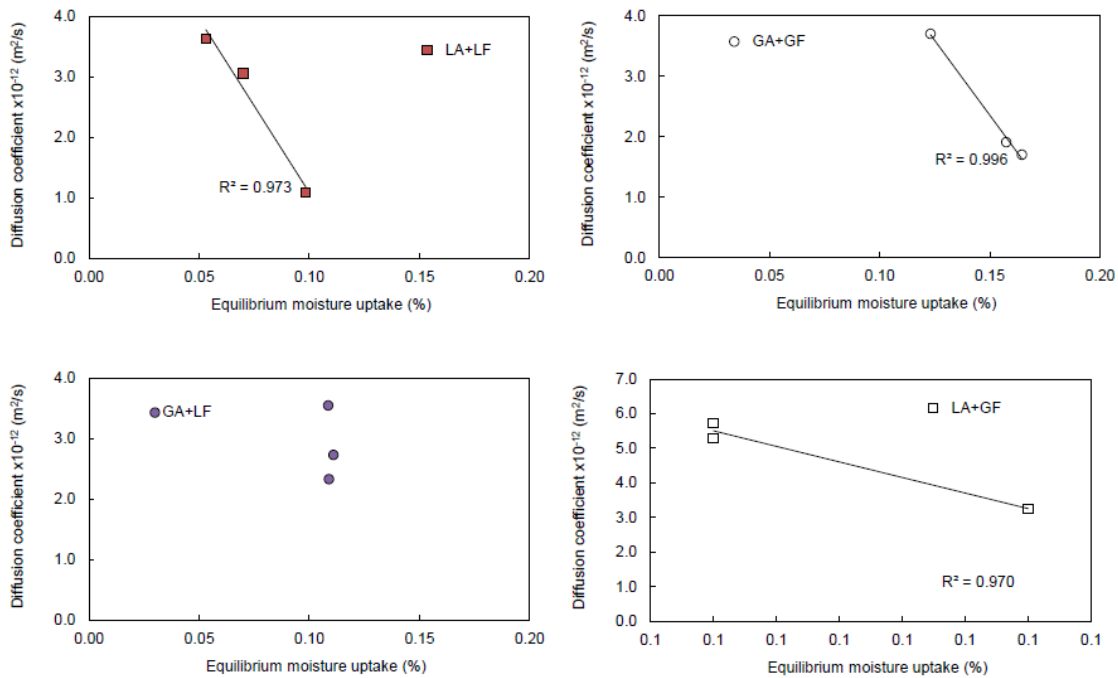
Fig. 6. Effects of aggregate type and specimen thickness on moisture diffusion of asphalt mastics containing the same limestone mineral filler (LF).



640 Fig. 7. Effects of mineral filler type on asphalt mastic diffusion coefficient. For the same aggregate type (limestone,  
 641 LA; or granite, GA, neither the limestone filler (LF) nor the granite filler (GF) significantly altered moisture  
 642 diffusion in asphalt mastic.  
 643  
 644  
 645

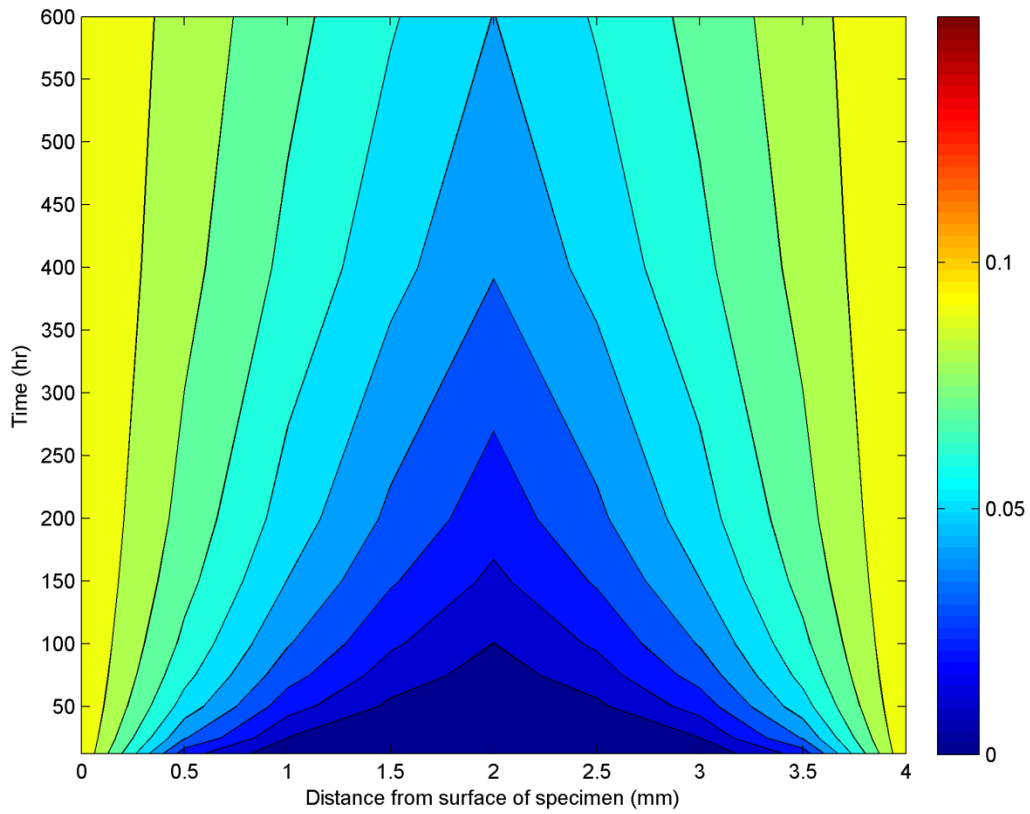


646  
 647 Fig. 8. Investigation of radial and longitudinal diffusion in asphalt mastic. Linear relationship between diffusion and  
 648 thickness suggest both modes of diffusion occurs in mastics.  
 649

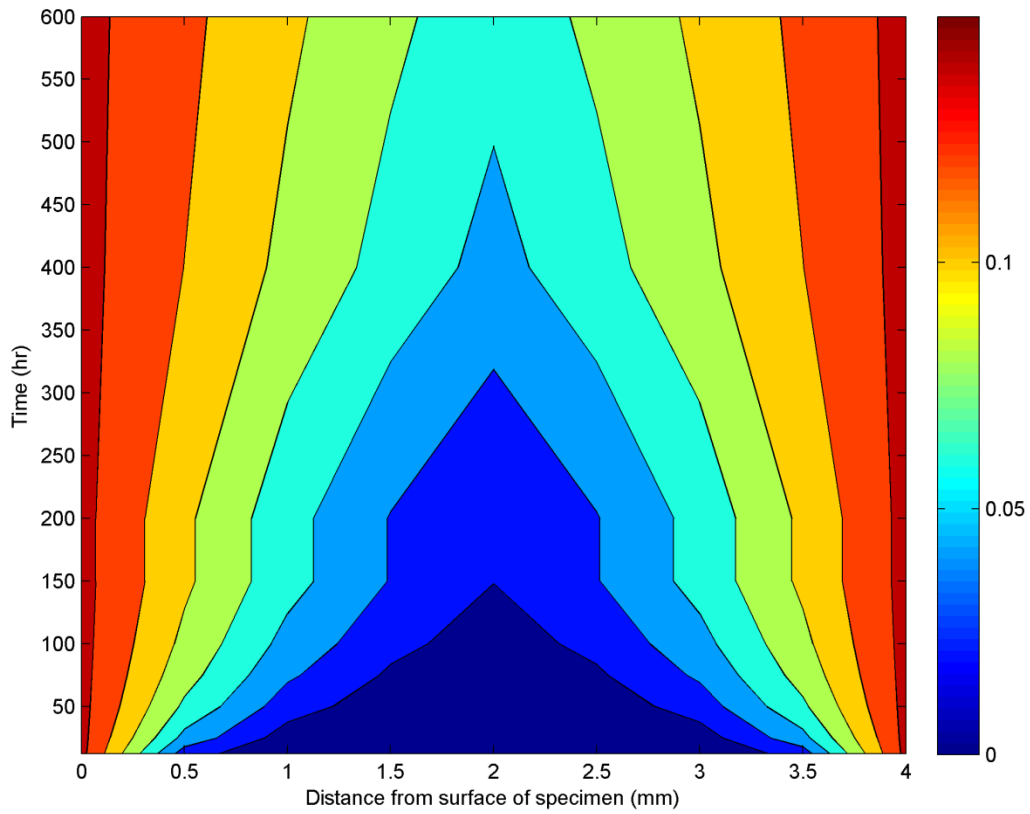


650  
 651 Fig. 9. Plots of diffusion coefficient against equilibrium moisture uptake showing linearly decreasing diffusivity  
 652 with moisture content for four different asphalt mastic types. The results demonstrate moisture diffusion in asphalt  
 653 mastic is concentration dependent.  
 654





655 Fig. 10. Simulation of moisture diffusion in asphalt mastic containing limestone aggregate and limestone filler.  
 656 Testing conditions simulated included 85% RH at a temperature of 23°C for moisture content ranging from about 0  
 657 to 0.10%. Plotted values are moisture uptake (%).  
 658



659 Fig. 11. Simulation of moisture diffusion in asphalt mastic containing granite aggregate and granite filler. Testing  
 660 conditions simulated included 85% RH at a temperature of 23°C for moisture content ranging from about 0 to  
 661 0.15%. Plotted values are moisture uptake (%).  
 662

663  
 664